





Role of Ciliary Protein Intraflagellar Transport Protein 88 in the Regulation of Cartilage Thickness and Osteoarthritis Development in Mice

Clarissa R. Coveney,  Linyi Zhu,  Jadwiga Miotla-Zarebska, Bryony Stott, Ida Parisi, Vicky Batchelor, Claudia Duarte, Emer Chang,  Eleanor McSorley, Tonia L. Vincent,  and Angus K. T. Wann

Objective. Mechanical and biologic cues drive cellular signaling in cartilage development, health, and disease. Primary cilia proteins, which are implicated in the transduction of biologic and physiochemical signals, control cartilage formation during skeletal development. This study was undertaken to assess the influence of the ciliary protein intraflagellar transport protein 88 (IFT88) on postnatal cartilage from mice with conditional knockout of the *Ift88* gene (*Ift88*-KO).

Methods. *Ift88^{fl/fl}* and *aggrecanCre^{ERT2}* mice were crossed to create a strain of cartilage-specific *Ift88*-KO mice (*aggrecanCre^{ERT2};Ift88^{fl/fl}*). In these *Ift88*-KO mice and *Ift88^{fl/fl}* control mice, tibial articular cartilage thickness was assessed by histomorphometry, and the integrity of the cartilage was assessed using Osteoarthritis Research Society International (OARS) damage scores, from adolescence through adulthood. In situ mechanisms of cartilage damage were investigated in the microdissected cartilage sections using immunohistochemistry, RNAScope analysis, and quantitative polymerase chain reaction. Osteoarthritis (OA) was induced in *aggrecanCre^{ERT2};Ift88^{fl/fl}* mice and *Ift88^{fl/fl}* control mice using surgical destabilization of the medial meniscus (DMM). Following tamoxifen injection and DMM surgery, the mice were given free access to exercise on a wheel.

Results. Deletion of *Ift88* resulted in progressive reduction in the thickness of the medial tibial cartilage in adolescent mice, as well as marked atrophy of the cartilage in mice during adulthood. In *aggrecanCre^{ERT2};Ift88^{fl/fl}* mice at age 34 weeks, the median thickness of the medial tibial cartilage was 89.42 μ m (95% confidence interval [95% CI] 84.00–93.49), whereas in *Ift88^{fl/fl}* controls at the same age, the median cartilage thickness was 104.00 μ m (95% CI 100.30–110.50; $P < 0.0001$). At all time points, the median thickness of the calcified cartilage was reduced. In some mice, atrophy of the medial tibial cartilage was associated with complete, spontaneous degradation of the cartilage. Following DMM, *aggrecanCre^{ERT2};Ift88^{fl/fl}* mice were found to have increased OARS scores of cartilage damage. In articular cartilage from maturing mice, atrophy was not associated with obvious increases in aggrecanase-mediated destruction or chondrocyte hypertrophy. Of the 44 candidate genes analyzed, only *Tcf7l2* expression levels correlated with *Ift88* expression levels in the microdissected cartilage. However, RNAScope analysis revealed that increased hedgehog (Hh) signaling (as indicated by increased expression of *Gli1*) was associated with the reductions in *Ift88* expression in the tibial cartilage from *Ift88*-deficient mice. Wheel exercise restored both the articular cartilage thickness and levels of Hh signaling in these mice.

Conclusion. Our results in a mouse model of OA demonstrate that IFT88 performs a chondroprotective role in articular cartilage by controlling the calcification of cartilage via maintenance of a threshold of Hh signaling during physiologic loading.

Supported by Versus Arthritis (grants 20205 and 21621). Dr. Coveney's work was supported by the Kennedy Trust for Rheumatology Research (grant KENN181907). Dr. Zhu's work was supported by the European Research Council (grant 743016). Ms. Chang's work was supported by the St. Hughs College, University of Oxford (Student Summer Research award). Ms. McSorley's work was supported by the Magdalen College, University of Oxford (Student Summer Research award). Dr. Wann's work was supported by the Kennedy Trust for Rheumatology Research (KTRR Fellowship).

Clarissa R. Coveney, DPhil (current address: Peabody Museum, Cambridge, Massachusetts), Linyi Zhu, PhD, Jadwiga Miotla-Zarebska, PhD, Bryony

Stott, PhD, Ida Parisi, PhD, Vicky Batchelor, MSc, Claudia Duarte, BSc, Emer Chang, BSc, Eleanor McSorley, BSc, Tonia L. Vincent, MD, PhD, Angus K. T. Wann, PhD: University of Oxford, Oxford, UK.

Dr. Vincent has received consulting fees from Mundipharma and GlaxoSmithKline (less than \$10,000 each). No other disclosures relevant to this article were reported.

Address correspondence to Clarissa R. Coveney, DPhil, Peabody Museum, 5th floor, 11 Divinity Avenue, Cambridge, MA 02138. Email: coveney.coxswain@gmail.com.

Submitted for publication February 2, 2021; accepted in revised form June 3, 2021.

INTRODUCTION

Articular cartilage absorbs and transmits mechanical loads generated by muscle contraction and weight-bearing during physical activity. Cartilage can be broadly divided into a noncalcified zone and a calcified zone adjacent to bone. Total cartilage thickness is allometrically scaled to the size of the organism, ensuring that chondrocytes experience similar force irrespective of the mass of the individual animal (1). Articular cartilage is extremely mechanosensitive, with chondrocytes closely monitoring and remodeling the extracellular matrix in response to physiologic loading (2,3). Physiologic mechanics are critical for cartilage development and homeostasis (4), since their loss has been demonstrated to lead to cartilage thinning (atrophy) (5,6).

Pathologic, supraphysiologic mechanical loading leads to the development of osteoarthritis (OA), in which degradation of the cartilage occurs, resulting in a loss of integrity of the articular surface (6). Cellular responses to mechanical force include the release of fibroblast growth factor receptor type 2 and transforming growth factor β (TGF β) from the matrix upon application of a mechanical load, as well as activation of a hedgehog (Hh) ligand, Indian hedgehog (7–10). A number of other pathways are implicated in cellular mechanotransduction, including connexin and ion channel opening and integrin activation. It is not yet understood how chondrocytes in cartilage integrate these cues as the cartilage matures through adolescence and as adaptation occurs to prepare for lifelong loading.

As in most cells in the body, articular chondrocytes express a single immotile primary cilium (11), a microtubule-based organelle reliant on intraflagellar transport (IFT) proteins, including IFT88. Components of the Hh pathway localize to the cilium, supporting bidirectional modulation of signaling (12). Cilia have been directly linked with other growth factor–signaling pathways such as TGF β signaling, and have also been indirectly linked with a large, growing list of signaling pathways (13), many of which are pertinent to cartilage health. The primary cilium has also been implicated as a “mechanosensory” structure (14). Findings from in vitro experiments in chondrocytes have implied that ciliary protein IFT88 is associated with both compression-induced production of extracellular matrix proteins (15) and impaired clearance of aggrecanases, resulting in exacerbated aggrecan degradation (16).

Developmental mutations in ciliary genes, including *Ift88*, result in impaired embryonic patterning as a result of disrupted Hh signaling (17). Cartilage-specific deletion of *Ift88* results in disrupted long bone and articular cartilage formation (18). Cartilage-specific deletion of *Ift80* in mice in the first 2 weeks of postnatal life was found to result in thickening of the articular cartilage (19). However, despite its putative influence over a range of processes that regulate health and disease in cartilage, we have very limited direct knowledge regarding the postdevelopmental influence of

ciliary IFT. We hypothesized that in a mouse model, ciliary protein IFT88 plays a crucial role in mediating cartilage homeostasis in adult animals.

MATERIALS AND METHODS

Animals. *Ift88*^{fl/fl} mice were obtained from The Jackson Laboratory (stock no. 022409) and were maintained as the control line. In parallel, offspring were crossed with *aggrecanCre*^{ERT2} mice, to generate *aggrecanCre*^{ERT2};*Ift88*^{fl/fl} mice (i.e., *Ift88*-knockout [*Ift88*-KO]), a mouse line that was originally generated at the Kennedy Institute of Rheumatology (20). The tdTomato reporter mouse line *B6.Cg-Gt(ROSA)26Sor^{tm14(CAG-tdTomato)Hze}/J* was used to confirm tissue-specific Cre recombination (stock no. 007914; The Jackson Laboratory). For all experiments, apart from destabilization of the medial meniscus (DMM) and wheel exercise (in which only male mice were used), both sexes were analyzed. No effect of sex was observed.

Tamoxifen treatment. Tamoxifen (product no. T5648; Sigma-Aldrich) was dissolved using sonication in 90% sunflower oil and 10% ethanol at a concentration of 20 mg/ml. Tamoxifen was administered by intraperitoneal injection at a dose of 50–100 mg/kg (according to the weight of the individual animal) on 3 consecutive days (*aggrecanCre*^{ERT2};*Ift88*^{fl/fl}, *Ift88*^{fl/fl}, and *aggrecanCre*^{ERT2};*tdTomato* mice; *n* = 5–22 per group) stratified by age (4, 6, or 8 weeks of age).

DMM. Mice were given tamoxifen 2 weeks prior to surgery. Male *Ift88*^{fl/fl} control mice and *aggrecanCre*^{ERT2};*Ift88*^{fl/fl} mice underwent DMM surgery at 10 weeks of age, as previously described (21), or underwent a capsulotomy as sham surgery. Thereafter, the mice were anesthetized using a previously described method (22) and then killed at 8 or 12 weeks after DMM (at 8 weeks, *n* = 14 *Ift88*^{fl/fl} mice and *n* = 12 *aggrecanCre*^{ERT2};*Ift88*^{fl/fl} mice; at 12 weeks, *n* = 15 *Ift88*^{fl/fl} mice and *n* = 15 *aggrecanCre*^{ERT2};*Ift88*^{fl/fl} mice).

Histology. Knee joints from the mice were harvested into 10% neutral buffered formalin (CellPath). The joints were then decalcified (in EDTA), paraffin embedded, and cut coronally through the entire depth of the joint. Sections (4 μ m in thickness) were stained with Safranin O at 80- μ m intervals.

Osteoarthritis Research Society International (OARSI) scoring. Safranin O–stained joint sections were assessed using a scoring system for severity of cartilage damage, as described previously (21). OARSI scores were assessed by 2 observers (CRC and IP) who were blinded with regard to the mouse group. The summed score method was used (the sum of the 3 highest scores per section, per joint, with a minimum of 9 sections per joint).

Osteophyte quantification. Osteophyte size and maturity, as well as loss of medial tibial cartilage proteoglycan staining, were assessed using a 0–3 scale, as previously described (23).

Cartilage thickness measurements. Thickness measurements were obtained from the mean of 3 measurements from both the medial and lateral tibial plateaus (total of 6 measurements), from 3 consecutive sections in the middle of the joint (total of 18 measurements). The same method was used to measure noncalcified cartilage thickness from the same location from which the total cartilage thickness measurement was obtained. Calcified cartilage thickness was calculated by subtracting the noncalcified cartilage thickness from the total cartilage thickness. All images were independently scored twice; measurements were obtained using ImageJ software (Supplementary Figure 1A, available on the *Arthritis & Rheumatology* website at <http://onlinelibrary.wiley.com/doi/10.1002/art.41894/abstract>).

Subchondral bone measurements. Subchondral bone measurements were obtained using a previously described method (24). Briefly, using ImageJ software, 5 measurements were obtained perpendicular to the articular cartilage plateau, from the chondro–osseous junction to the top of the bone marrow or to the growth plate if there was no bone marrow. Thickness was measured in ≥ 3 sections of each plateau of each knee.

Micro-computed tomography (micro-CT) analysis of bone volume/total volume (BV/TV). Mouse knee joints were scanned using a SkyScan 1172 Micro-CT apparatus in 70% ethanol (10 $\mu\text{m}/\text{pixel}$). A 3-dimensional analysis was used to examine parameters including tissue and bone volume, tissue and bone surface area, trabecular thickness, separation, and volume, and trabecular pattern factor, measured using CTAn (Bruker).

Immunohistochemistry (IHC). Unstained fixed, decalcified coronal sections of the knee joints were deparaffinized, rehydrated, and quenched in 0.3M glycine and treated with proteinase K for 10 minutes. Tissue sections were treated with chondroitinase (0.1 units) for 30 minutes at 37°C, blocked in 5% goat serum and 10% bovine serum albumin in phosphate buffered saline, and permeabilized with 0.2% Triton X-100 for 15 minutes. The cartilage was then incubated overnight at 4°C with one of the following primary antibodies: anti-type X collagen in a 1:50 ratio (product no. ab58632; Abcam), anti-NITEGE in a 1:50 ratio (product no. PA1-1746; Thermo Scientific), IgG control in a 1:50 ratio, or no primary antibody. Sections were washed and incubated with Alexa Fluor 555 secondary antibodies for 30 minutes. Cartilage samples were incubated with the nuclear stain DAPI (in a 1:5,000 ratio), before being mounted in Prolong Gold.

RNA extraction. Articular cartilage was microdissected from the femoral and tibial plateaus using a scalpel (each data point from 2 animals) and was harvested directly into RNeasy lysis buffer (Qiagen). Samples were transferred to RLT buffer (Qiagen) and were diced before pulverization using a PowerGen 125 Polytron instrument (Fisher Scientific) (3 times for 20 seconds each). RNA in mouse knee cartilage was isolated using an RNeasy micro kit (Qiagen).

Quantitative polymerase chain reaction (qPCR). Using RNA isolated from microdissected knee cartilage, complementary DNA was synthesized (Applied Biosystems) and real-time qPCR was performed using a ViiA 7 real-time PCR instrument on 384 custom-made TaqMan microfluidic cards (product no. 4342253; ThermoFisher). Threshold cycle values were normalized to the mean values for *Gapdh* and *Hprt*. Linear regression analyses were used to assess correlations with *Ift88* expression, and subsequently raw *P* values and corrected *P* (P_{corr}) values (Bonferroni adjusted) were calculated using GraphPad Prism software version 9.

RNAScope analysis. Knee joints were harvested into ice-cold 4% paraformaldehyde and incubated in a refrigerated environment for 24 hours before being transferred into ice-cold 10%, 20%, and 30% sucrose, each for 24 hours. RNAScope probes Mm-Ift88-C1 (product no. 420211-C1) and Mm-Gli1-C2 (product no. 311001-C2) were used in combination with Opal 570 reagent pack signals (product no. FP14880001KT) and 690 reagent pack signals (product no. FP1497001KT) (all from ACD inc.), with the values normalized to those of both positive and negative controls. For further details on slide preparation and more information regarding the imaging protocols applied when using the RNAScope multiplex fluorescent reagent kit version 2 (product no. 323100), see Supplementary Methods (available on the *Arthritis & Rheumatology* website at <http://onlinelibrary.wiley.com/doi/10.1002/art.41894/abstract>).

RESULTS

Thinner medial articular cartilage in adolescent mice following *Ift88* deletion in chondrocytes. To confirm inducible tissue-specific Cre recombination, the *aggrecan*^{Cre^{ERT2}} mouse line was crossed with a tdTomato reporter mouse line, and tamoxifen was administered at 4 and 8 weeks of age. Two weeks following tamoxifen treatment, activation of Cre recombinase was observed in superficial hip articular cartilage chondrocytes (Supplementary Figure 2A, available on the *Arthritis & Rheumatology* website at <http://onlinelibrary.wiley.com/doi/10.1002/art.41894/abstract>), as well as in knee articular cartilage chondrocytes and menisci ($n = 3$) (Figure 1A).

In mice, throughout adolescence and adulthood, articular cartilage was thicker on the medial tibial plateau than on the lateral

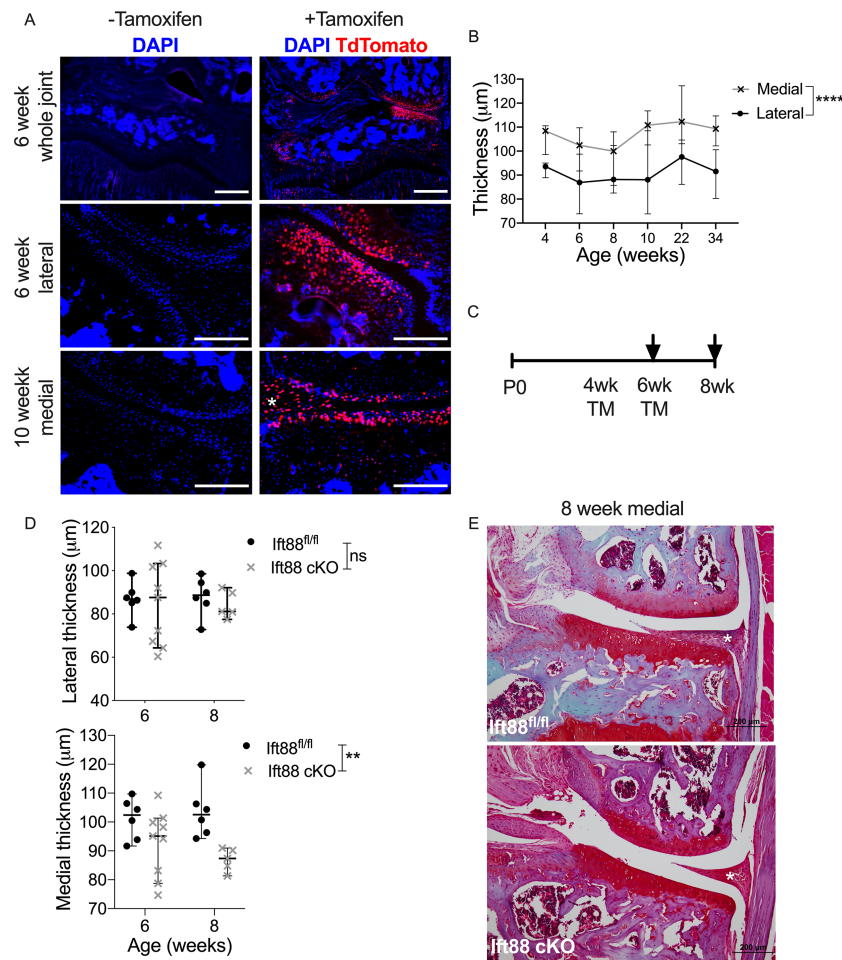


Figure 1. Deletion of *Ift88* in adolescent mice leads to thinner articular cartilage. **A** and **C**, *AggrecanCre^{ERT2}; tdTomato* mice were left untreated or treated with tamoxifen (TM) at ages 4 weeks or 8 weeks (as illustrated by the diagram in **C**; arrows indicate sample collection points), and cryosections of the whole knee joint and the medial and lateral compartments were obtained for immunofluorescence analysis (counterstained with DAPI) (**A**). Bars = 200 μm. **B** and **D**, Thickness of the medial and lateral articular cartilage was assessed in sections from control mice at ages 4, 6, 8, 10, 22, and 34 weeks (**B**), and from *aggrecanCre^{ERT2}; Ift88^{fl/fl}* (*Ift88*–conditional knockout [cKO]) mice and *Ift88^{fl/fl}* control mice at ages 6 weeks or 8 weeks (**D**). Symbols represent individual mice; bars show the median ± 95% confidence interval. ** = $P < 0.01$; **** = $P < 0.0001$, by two-way analysis of variance. **E**, Images show Safranin O staining of the cartilage from the medial meniscus of a representative *Ift88^{fl/fl}* mouse and *Ift88*-cKO mouse at age 8 weeks, 2 weeks after tamoxifen injection. The white asterisk in **A** and **E** indicates the medial meniscus. NS = not significant.

plateau ($P < 0.0001$) (Figure 1B). *Ift88* was deleted at 4 or 6 weeks of age, and analysis was conducted 2 weeks later (Figure 1C). Deletion of *Ift88* in mice at age 6 weeks resulted in reduced thickness of the medial and lateral knee cartilage, which was significantly different compared to that in the control group (median 82.96 μm [95% confidence interval (95 CI) 81.13–91.56] in *aggrecanCre^{ERT2}; Ift88^{fl/fl}* mice versus 95.58 μm [95% CI] 92.08–99.68] in control mice). A similar effect was not observed when *Ift88* was deleted at 4 weeks of age (Supplementary Figure 2B, available on the *Arthritis & Rheumatology* website at <http://onlinelibrary.wiley.com/doi/10.1002/art.41894/abstract>). Considering each plateau separately, deletion of *Ift88* in mice resulted in a significant reduction in medial cartilage thickness at 6 weeks of age (median thickness 102.42 μm [95% CI 91.7–109.7] in control mice and 94.25 μm [95% CI 78.7–101.3] in

aggrecanCre^{ERT2}; Ift88^{fl/fl} mice) and at 8 weeks of age (median thickness 102.57 μm [95% CI 94.3–119.8] in control mice and 87.36 μm [95% CI 81.35–90.97] in *aggrecanCre^{ERT2}; Ift88^{fl/fl}* mice) (Figures 1D and E). Lateral cartilage thickness was unaffected (Figure 1D).

Thinner calcified articular cartilage resulting from *Ift88* deletion. In a previous mouse study, reduced thickness of the articular cartilage was associated with acceleration of programmed hypertrophy upon postnatal activation of Hh signaling in mice (25). To assess the effects of *Ift88* deletion on cartilage in maturing mice, we measured the thickness of noncalcified and calcified cartilage (Figure 2A and Supplementary Figure 1A, available on the *Arthritis & Rheumatology* website at <http://onlinelibrary.wiley.com/doi/10.1002/art.41894/abstract>). In control mice, the

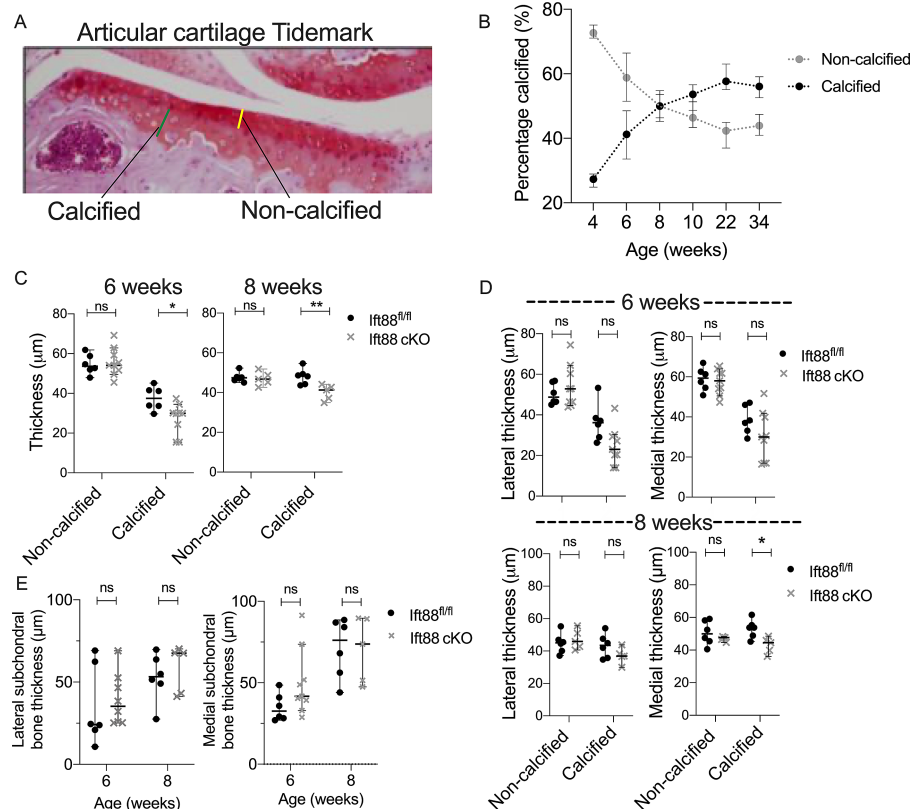


Figure 2. Deletion of *Ift88* in adolescent mice leads to thinner calcified articular cartilage. **A** and **B**, Sections of knee articular cartilage from mice were stained with Safranin O to identify the noncalcified and calcified areas of the cartilage (demarcated by the tidemark) (**A**), and to determine the median percentage of cartilage that was calcified versus noncalcified in sections from mice at different ages ($n = 3$ for 4-week-old mice; $n = 6$ – 19 for all other age groups) (**B**). **C** and **D**, Thickness of the noncalcified and calcified areas of the articular cartilage was compared between *aggrecan-Cre^{ERT2};Ift88^{fl/fl}* (*Ift88*-cKO) mice and *Ift88^{fl/fl}* control mice at ages 6 weeks or 8 weeks, in the whole joint (**C**) or by medial and lateral compartment (**D**). **E**, Median subchondral bone thickness was compared between *aggrecan-Cre^{ERT2};Ift88^{fl/fl}* (*Ift88*-cKO) mice and *Ift88^{fl/fl}* control mice at ages 6 weeks or 8 weeks. Symbols represent individual mice; bars show the median \pm 95% confidence interval. A minimum of 5 joints was assessed in any group. * = $P < 0.05$; ** = $P < 0.01$, by two-way analysis of variance. See Figure 1 for definitions.

proportion of calcified articular cartilage increased from 25% at 4 weeks of age to 60% by 22 weeks of age (Figure 2B). Deletion of *Ift88* resulted in thinner calcified cartilage at 6 weeks of age (median thickness 37.52 μm [95% CI 29.71–45.17] in control mice and 29.96 μm [95% CI 15.46–34.50] in *aggrecan-Cre^{ERT2};Ift88^{fl/fl}* mice) and at 8 weeks of age (median thickness 48.43 μm [95% CI 43.62–54.64] in control mice and 41.29 μm [95% CI 34.93–44.17] in *aggrecan-Cre^{ERT2};Ift88^{fl/fl}* mice), though these reductions were only statistically significant on the medial plateau (Figure 2C). Separating measurements by lateral and medial plateaus revealed reductions in calcified cartilage that were observable across both plateaus and time points, though these reductions were only significant on the medial plateau at 8 weeks of age (Figure 2D).

Histologic measurements of the subchondral bone (Supplementary Figure 1B, available on the *Arthritis & Rheumatology* website at <http://onlinelibrary.wiley.com/doi/10.1002/art.41894/abstract>) revealed that bone thickness approximately doubled between 6 and 8 weeks of age in control mice (Figure 2E). However, deletion of *Ift88* did not result in enhanced bone

thickening. Additionally, there was no tartrate-resistant acid phosphatase staining (Supplementary Figure 1C) in the articular cartilage or the bone beneath, suggesting very little osteoclast activity in the calcified cartilage or subchondral bone at these time points.

Association of reductions in calcified cartilage thickness with articular cartilage atrophy following *Ift88* deletion in mice at 8 weeks of age. Progressive calcification of articular cartilage continued when mice were between 8 and 22 weeks of age (Figure 2B). Tamoxifen was administered at 8 weeks of age, and joints were collected at 10, 22, and 34 weeks of age (Figure 3A). Deletion of *Ift88* resulted in a 10–20% reduction in the thickness of tibial cartilage at every time point (Figures 3B and C). Based on the mean values across both plateaus, thinning was not cumulative over time and occurred without obvious surface fibrillation, thus representative of atrophy rather than degeneration (3,5,26,27). At 22 and 34 weeks of age, thinning of the medial plateau of *Ift88*-KO mice was significantly greater than

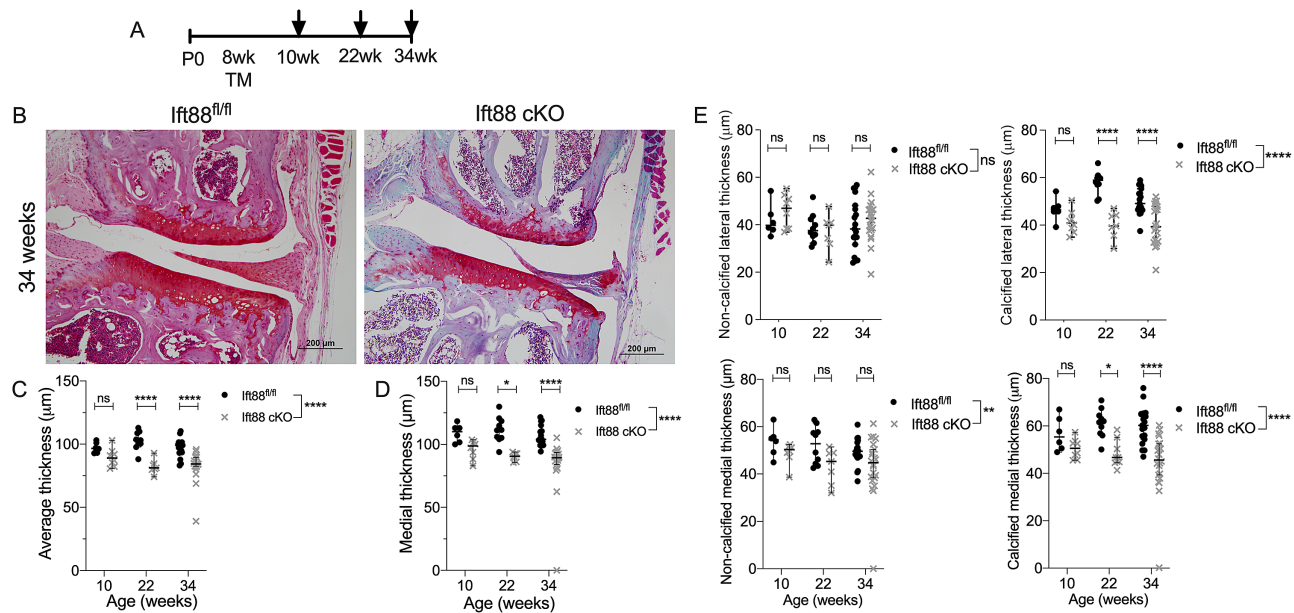


Figure 3. Deletion of *Ift88* in mice at age 8 weeks results in atrophy of the articular cartilage and reduced thickness of the calcified cartilage. **A**, Experimental timeline shows the age of the mice when tamoxifen was injected and the time points when tissue samples were collected (arrows). **B**, Sections of medial articular cartilage from 34-week-old *Ift88* control and *aggrecanCre^{ERT2};Ift88^{fl/fl}* (*Ift88*-cKO) mice were stained with Safranin O for histologic analysis. **C** and **D**, In *Ift88^{fl/fl}* controls and *Ift88*-cKO mice at each age, thickness of the articular cartilage was measured in both the medial and lateral compartments (**C**) and in the medial compartment alone (**D**). **E**, Thickness of the noncalcified and calcified areas of the articular cartilage in both the lateral and medial compartments was compared between groups of mice at each age. Symbols represent individual mice; bars show the median \pm 95% confidence interval. * = $P < 0.05$; ** = $P < 0.01$; **** = $P < 0.0001$, by two-way analysis of variance. See Figure 1 for definitions.

that of control mice. By the time the mice reached 34 weeks of age, the median thickness of the medial plateau was 104.00 μ m (95% CI 100.30–110.50) in control mice and 89.42 μ m (95% CI 84.00–93.49) in *aggrecanCre^{ERT2};Ift88^{fl/fl}* mice (Figure 3D). Atrophy was milder on the lateral tibial plateaus and was not apparent until mice reached 22 weeks of age (Supplementary Figure 3A, available on the *Arthritis & Rheumatology* website at <http://onlinelibrary.wiley.com/doi/10.1002/art.41894/abstract>).

The effect of *Ift88* deletion on the thickness of the noncalcified cartilage was not statistically significant on either the medial or the lateral plateaus (Figure 3E). In contrast, statistically significant reductions in the thickness of the calcified cartilage were observed on both the medial and the lateral plateaus (medial plateau, median 58.72 μ m [95% CI 54.34–65.05] in control mice versus 45.62 μ m [95% CI 39.32–52.49] in *aggrecanCre^{ERT2};Ift88^{fl/fl}* mice) (Figure 3E).

Prior evidence has shown that cartilage thinning and accelerated hypertrophy occur in association with reduced numbers of chondrocytes in articular cartilage following reactivation with Hh signaling (25). However, no significant reductions in cell number or density were observed in 10-week-old *aggrecanCre^{ERT2};Ift88^{fl/fl}* mice (Supplementary Figure 3B, available on the *Arthritis & Rheumatology* website at <http://onlinelibrary.wiley.com/doi/10.1002/art.41894/abstract>). TUNEL staining revealed limited apoptosis in both control mice and *aggrecanCre^{ERT2};Ift88^{fl/fl}* mice (Supplementary Figure 3C).

Predisposition of joints to spontaneous OA following atrophy of the medial tibial cartilage.

At 34 weeks of age, *aggrecanCre^{ERT2};Ift88^{fl/fl}* mice developed spontaneous cartilage damage in the medial compartment and this was found to be associated with osteophyte formation, indicating the development of OA (Figure 4A). OARSI scoring revealed a significant increase in cartilage damage scores when mice were 34 weeks of age (Figure 4B), but no significant increase when mice were 22 weeks of age (Supplementary Figure 4A, available on the *Arthritis & Rheumatology* website at <http://onlinelibrary.wiley.com/doi/10.1002/art.41894/abstract>). The highest OARSI scores were found on the medial plateau (Figure 4C). There was no difference in osteophyte scores, except in cartilage displaying severe damage (Figure 4D and Supplementary Figure 4B, <http://onlinelibrary.wiley.com/doi/10.1002/art.41894/abstract>). There were no changes in subchondral bone thickness following *Ift88* deletion in mice at either 10 or 22 weeks of age. By 34 weeks of age, cartilage thinning was associated with a loss of subchondral bone in *aggrecanCre^{ERT2};Ift88^{fl/fl}* mice (Figure 4E and Supplementary Figure 4C, <http://onlinelibrary.wiley.com/doi/10.1002/art.41894/abstract>). Trabecular bone density (BV/TV) in the epiphysis was not affected by deletion of *Ift88* (Supplementary Figure 4D).

Exacerbation of OA severity after surgical joint destabilization and deletion of *Ift88*. Mice were given tamoxifen at 8 weeks of age, and surgical DMM was performed

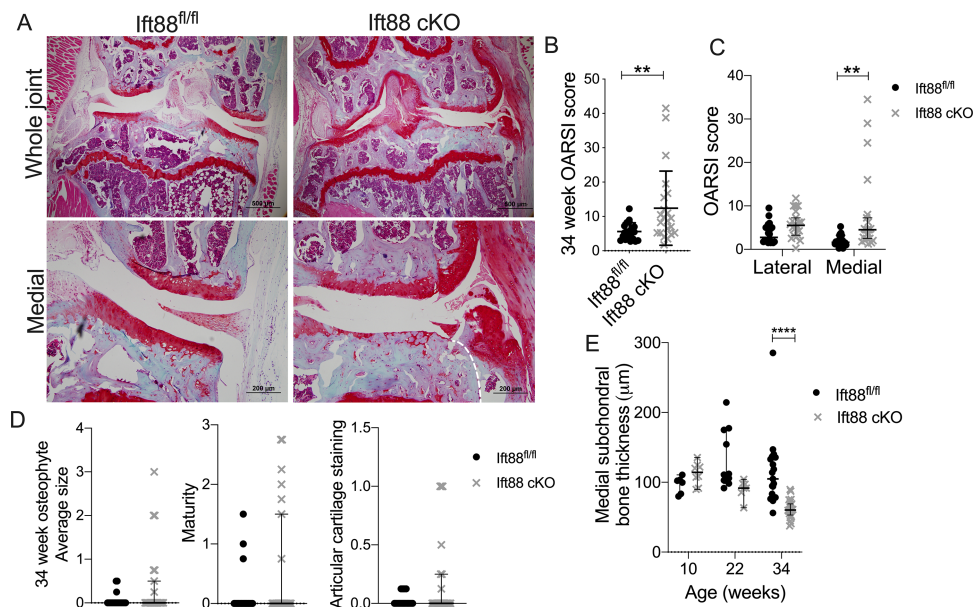


Figure 4. Features of spontaneous osteoarthritis (OA) in *Ift88*-conditional knockout [cKO] mice at age 34 weeks. **A**, Whole joint sections and sections from the medial compartment of the articular cartilage from 34-week-old *Ift88*^{fl/fl} control and *Ift88*-cKO mice were stained with Safranin O for histologic analysis of OA-like features. The **curved white broken line** in the bottom right panel indicates the area of osteophyte formation. **B** and **C**, Summed modified Osteoarthritis Research Society International (OARSJ) scores were used to assess joint damage in articular cartilage sections from 34-week-old *Ift88*^{fl/fl} control and *Ift88*-cKO mice, in the whole joint (**B**) and by compartment (**C**). ** = $P < 0.01$ by Mann-Whitney test. **D**, Articular cartilage from 34-week-old *Ift88*^{fl/fl} control and *Ift88*-cKO mice was assessed for median osteophyte size and maturity, as well as for osteophyte staining scores. **E**, Thickness of the subchondral bone was assessed in the medial compartment of articular cartilage from *Ift88*^{fl/fl} control and *Ift88*-cKO mice at ages 10, 22, or 34 weeks. Symbols represent individual mice (19–22 mice per group); bars show the median \pm 95% confidence interval. **** = $P < 0.0001$ by two-way analysis of variance.

at 10 weeks of age. At either 8 or 12 weeks after surgery, mice were killed and the knee joints were collected, including those from sham-operated mice at the same time points (Figure 5A). Coronal histologic joint sections (Figure 5B) were assessed using summed OARSJ scores of cartilage damage. Deletion of *Ift88* resulted in exacerbated disease activity 12 weeks after DMM (mean \pm SD OARSJ score 22.08 ± 9.30 in *Ift88*^{fl/fl} mice versus 29.83 ± 7.69 in *aggrecanCre*^{ERT2};*Ift88*^{fl/fl} mice [$P < 0.05$]; $n = 15$ mice per group) (Figure 5C). No differences in osteophyte size (Figure 5D and Supplementary Figure 5A, available on the *Arthritis & Rheumatology* website at <http://onlinelibrary.wiley.com/doi/10.1002/art.41894/abstract>), osteophyte maturity, or osteophyte staining scores (Supplementary Figures 5B–E) were observed between control mice and *aggrecanCre*^{ERT2};*Ift88*^{fl/fl} mice at either time point after DMM. Further, we observed no difference in the BV/TV of the epiphysis between control mice and *aggrecanCre*^{ERT2};*Ift88*^{fl/fl} mice 12 weeks following DMM (Supplementary Figure 5F).

Lack of association between articular cartilage atrophy and markers of matrix catabolism or hypertrophy.

To assess whether *Ift88* deletion increased the catabolism of aggrecan, knee joints from control mice and *aggrecanCre*^{ERT2};*Ift88*^{fl/fl} mice were probed for protease-generated neopeptides as described previously (22), using an antibody raised against the

synthetic epitope NITEGE, and with an IgG antibody used as an isotype control (Supplementary Figure 6A, available on the *Arthritis & Rheumatology* website at <http://onlinelibrary.wiley.com/doi/10.1002/art.41894/abstract>). The NITEGE signal was weak in sections probed with the IgG positive control antibody (Supplementary Figure 6A), and no differences in NITEGE signaling were observed between the joints from control mice and joints from *aggrecanCre*^{ERT2};*Ift88*^{fl/fl} mice (Figure 6A). Moreover, no differences in *ColX* expression, a marker of Hh-driven chondrocyte hypertrophy (28), were observed between *Ift88*-KO mice and control mice, as determined by IHC (Figure 6B; results compared against the IgG control are shown in Supplementary Figure 6B).

Results of bulk RNA analyses implicating *Tcf7l2* in cartilage atrophy.

Two weeks after tamoxifen treatment, RNA was isolated from microdissected articular cartilage obtained from the knee joints of 10-week-old *Ift88*-KO and control mice (Supplementary Figure 6C, available on the *Arthritis & Rheumatology* website at <http://onlinelibrary.wiley.com/doi/10.1002/art.41894/abstract>). A total of 44 candidate genes, which were all either associated with chondrocyte biology and/or implicated in primary ciliary signaling, were measured using qPCR. Due to the mosaic Cre activity (Figure 1A) and sample pooling, we conducted a correlation analysis to assess correlations between *Ift88* expression and expression of the candidate

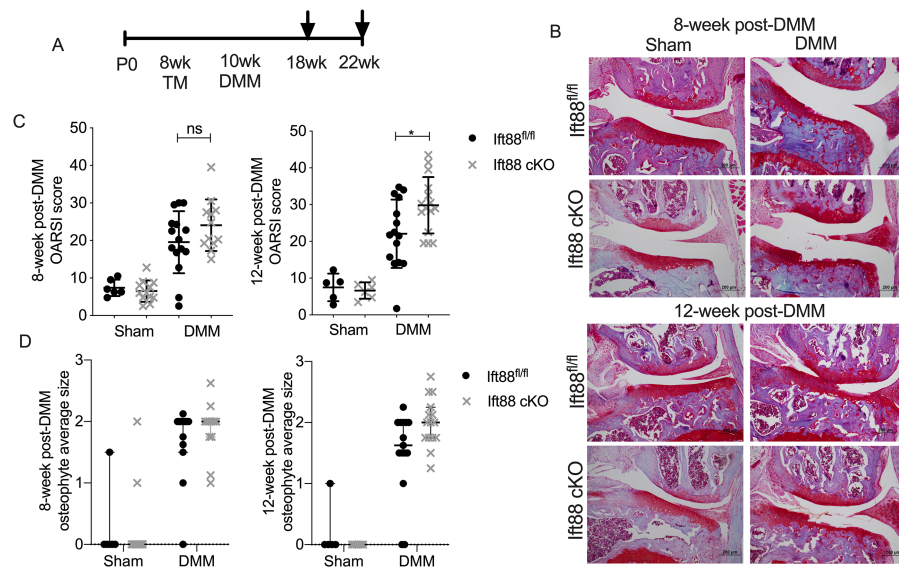


Figure 5. Deletion of *Ift88* in mice exacerbates disease at 12 weeks after surgical destabilization of the medial meniscus (DMM). **A**, Experimental timeline shows the time points for tamoxifen injection and DMM surgery, as well as sample collection (arrows). **B**, Joint sections from the medial compartment of the articular cartilage of sham-operated and DMM-operated *Ift88*^{fl/fl} control and *Ift88*-cKO mice, obtained at 8 weeks and 12 weeks after surgery, were stained with Safranin-O for histologic analysis. **C** and **D**, Articular cartilage from sham-operated mice (minimum of 5 mice per group) and DMM-operated mice (12–15 mice per group) were assessed for summed modified Osteoarthritis Research Society International (OARS1) joint damage scores (**C**) and median osteophyte size (**D**) at 8 weeks and 12 weeks after DMM. Symbols represent individual mice; bars show the median \pm 95% confidence interval. * = $P < 0.05$ by two-way analysis of variance. See Figure 1 for other definitions.

genes, with values normalized to the mean values for the 2 most stable housekeeping genes, *Hprt* and *Gapdh* (for all genes see Supplementary Table 1, available on the *Arthritis & Rheumatology* website at <http://onlinelibrary.wiley.com/doi/10.1002/art.41894/abstract>). Expression of the majority of candidate genes did not correlate with *Ift88*, including *Adamts5* and *ColX* (Supplementary Figure 6D), which was consistent with the IHC findings (Figures 6A and B). *Tcf7l2* (29) was the only gene found to be correlated with *Ift88* expression at a level that was statistically significant after Bonferroni correction ($P = 0.0006$, $P_{\text{corr}} = 0.026$, $r^2 = 0.8811$). Levels of *Ctgf*, *Tgfb3*, *Gli2*, and the regulator of cartilage calcification *Enpp1* (30) were positively correlated with *Ift88* expression before Bonferroni correction ($P = 0.002$, $P = 0.0107$, $P = 0.0037$, and $P = 0.009$, respectively) (Figure 6C and Supplementary Figure 6C, available on the *Arthritis & Rheumatology* website at <http://onlinelibrary.wiley.com/doi/10.1002/art.41894/abstract>), but not after Bonferroni correction. Expression of *Gli1* and *Ptch1*, indicators of Hh pathway activation, did not correlate with *Ift88* expression (Supplementary Table 1).

Reduction in *Ift88* expression in *aggrecanCre*^{ERT2}; *Ift88*^{fl/fl} mouse cartilage revealed using RNAScope analysis. To overcome the limitations of bulk RNA analyses, an RNAScope analysis was performed on cryosections of tibial articular cartilage from 10-week-old control and *aggrecanCre*^{ERT2}; *Ift88*^{fl/fl} mice ($n = 4$ each) to assess *Ift88* expression, in situ. Results of the RNAScope

analysis revealed that a mean of 39.61% of cells were positive for *Ift88* in control mouse cartilage in comparison to a mean of 27.78% of *Ift88*-positive cells in *aggrecanCre*^{ERT2}; *Ift88*^{fl/fl} mouse cartilage, indicating a 30% reduction in *Ift88*-positive cells ($P < 0.0001$ by Fisher's exact test) (Figure 6D; for images and contingency data for statistical comparisons, see Supplementary Figure 6E, available on the *Arthritis & Rheumatology* website at <http://onlinelibrary.wiley.com/doi/10.1002/art.41894/abstract>).

Effect of wheel exercise on cartilage atrophy and associated increases in Hh signaling in situ. RNAScope analysis was performed to investigate the expression of *Gli1*, a marker of Hh pathway activity, in the same cartilage sections in which reduced *Ift88* expression was observed. A mean total of 24.12% of nuclei were positive for *Gli1* in control mouse articular cartilage in comparison to a total of 45.46% of *Gli1*-positive nuclei in *aggrecanCre*^{ERT2}; *Ift88*^{fl/fl} mouse articular cartilage (Figure 6E). This increase in the percentage of *Gli1*-positive cells, indicative of increased Hh signaling, was statistically significant ($n = 4$ each; $P < 0.0001$) (for raw cell counts, see Supplementary Figure 6E, available on the *Arthritis & Rheumatology* website at <http://onlinelibrary.wiley.com/doi/10.1002/art.41894/abstract>). Analyzing *Gli1* in terms of signal per cell also revealed higher expression of *Gli1* in *aggrecanCre*^{ERT2}; *Ift88*^{fl/fl} mice (2.88 mean dots per cell per animal) compared to control mice (1.49 mean dots per cell per animal), representing a statistically significant difference ($n = 4$ each; $P < 0.01$) (Figure 6E).

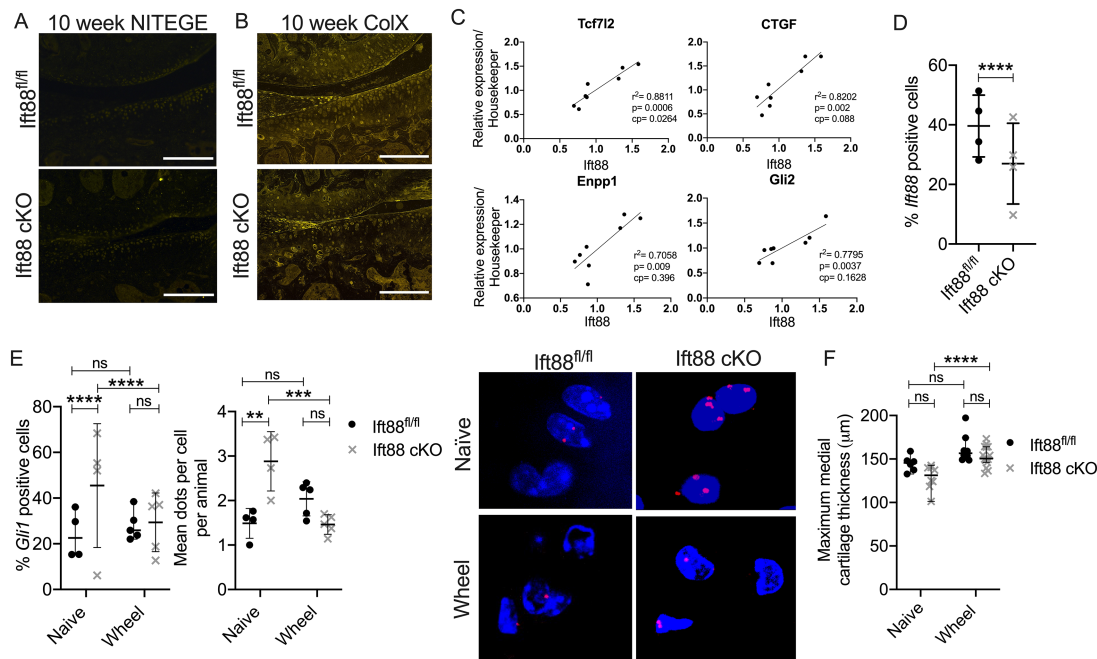


Figure 6. Wheel exercise rescues cartilage atrophy and suppresses increased hedgehog signaling in mouse chondrocytes. **A** and **B**, Immunofluorescence staining of articular cartilage chondrocytes from a representative *Ift88*^{fl/fl} control mouse and *Ift88*-cKO mouse at age 10 weeks shows expression of the aggrecan neoepitope NITEGE (**A**) and type X collagen (ColX) (**B**). Bars = 200 μm. **C**, RNA extracted from the microdissected articular cartilage was analyzed using quantitative polymerase chain reaction to identify genes showing a correlation with *Ift88* expression. Values were normalized to the mean values for the housekeeping genes *Gapdh* and *Hprt*. Linear regression analyses were performed, and significance was assessed before and after Bonferroni correction (corrected *P* [cp]). **D** and **E**, Findings from RNAScope analysis of the articular cartilage chondrocytes show the percentage of chondrocytes that were positive for *Ift88* expression in *Ift88*^{fl/fl} control and *Ift88*-cKO mice (**D**), and the percentage of *Gli1*-positive cells, mean number of *Gli1*-positive dots per cell per mouse, and number of *Gli1*-positive nuclei in *Ift88*^{fl/fl} control and *Ift88*-cKO exercise-naïve mice compared to wheel-exercised mice (**E**). ** = *P* < 0.01; *** = *P* < 0.001; **** = *P* < 0.0001, by two-way analysis of variance. **F**, Maximum medial cartilage thickness was compared between exercise-naïve and wheel-exercised *Ift88*^{fl/fl} control and *Ift88*-cKO mice. **** = *P* < 0.0001 by Fisher's exact test. Symbols represent individual mice; bars show the median ± 95% confidence interval. See Figure 1 for other definitions.

Mice were given free access to wheel exercise for 2 weeks immediately following the tamoxifen injection administered at 8 weeks of age (over the same time period that atrophy develops). In these experiments, no measurable difference in articular cartilage thickness was observed when comparing control mice to *aggrecanCre*^{ERT2};*Ift88*^{fl/fl} mice (Figure 6F and Supplementary Figure 6F, available on the *Arthritis & Rheumatology* website at <http://onlinelibrary.wiley.com/doi/10.1002/art.41894/abstract>). Wheel exercise did not affect the number of *Gli1*-positive cells or *Gli1* expression per cell in control mice, but, according to findings from both analyses, wheel exercise reduced *Gli1* expression in *aggrecanCre*^{ERT2};*Ift88*^{fl/fl} mice, effectively restoring Hh signaling and cartilage thickness to the levels observed in control mice.

DISCUSSION

In the current study, we explored the influence of ciliary protein IFT88 in postnatal mouse articular cartilage in vivo, by depleting its expression in chondrocytes at different stages of postnatal skeletal maturation. When *Ift88* was deleted in the mice at 4, 6,

and 8 weeks of age, we observed rapid cartilage thinning, largely in the calcified cartilage within the medial joint compartment. Thinning was determined to be indicative of atrophy rather than degeneration, since there was no disruption of the articular surface. However, as mice aged, cartilage atrophy was associated with increased severity of spontaneous OA and DMM-induced OA.

We speculate that the *Ift88*-dependent effects in the thicker medial compartment of the mouse joint are mechanically driven (6) in a manner analogous to the bone “mechanostat” proposed by Frost in 1987 (31). In essence, this model ensures that chondrocytes mechanoadapt the extracellular matrix so as to experience force within a narrow window (1). Since cartilage thickness can be restored in *Ift88*-conditional KO mice with wheel exercise, this suggests that ciliary protein IFT88 may influence, but is not solely responsible for, cartilage mechanoadaptation in vivo. Similar modes of action have been proposed in the context of epithelial response to renal flow (14,32). Our findings contrast with the observation that in mice, deletion of *Ift88* during development leads to increased cartilage thickness (17), possibly indicating a changing influence of *Ift88* with skeletal maturation.

Since atrophy in *Ift88*-conditional KO mice is largely restricted to calcified cartilage, we speculate that this represents a failure of cartilage hypertrophy during maturation, in a load-dependent manner. Cartilage thinning was not associated with increased matrix catabolism, enhanced subchondral bone thickness, osteoclast activity, or density changes (BV/TV) in the epiphysis, but we cannot exclude the possibility that calcified cartilage is transitioning to the bone in these mice. Calcification of mouse cartilage has recently been linked to *Enpp1*, a pyrophosphatase believed to inhibit calcification through Hh signaling (30). Findings from our molecular analyses indicated that *Enpp1* positively correlates with *Ift88* expression, indicating a reduction in the levels of an inhibitor of calcification in *Ift88*-conditional KO mice. This could result in accelerated ossification analogous to that seen in the growth plates of ciliary protein mutant mice and in articular cartilage upon postnatal activation of Hh (25).

Prior studies investigating congenital mutations (33) or constitutive deletions of *Ift88* (17,18,34) demonstrated that *Ift88* plays a role in mouse limb and joint development. Mouse models targeting other ciliary components, *Kif3a*, Bardet-Biedl syndrome proteins, and *Ift80*, also implicate ciliary machinery in musculoskeletal development (19,28). This influence over skeletal development is also exemplified by the human skeletal ciliopathies (35,36). The most important molecular pathway associated with ciliopathy is Hh, although other pathways have also been described (10,37–41). Hh signaling largely switches off in adulthood (42) but is reactivated in OA (8). We investigated the molecular basis of *Ift88*-dependent cartilage atrophy by identifying the correlation between *Ift88* expression (reflecting efficiency of deletion) and 44 molecules previously demonstrated to be associated with ciliary signaling and cartilage biology. In addition, we explored Hh signaling by directly visualizing *Gli1* expression in murine cartilage using RNAScope. The gene that correlated most strongly with ciliary signaling was transcription factor *Tcf7l2*, previously shown to influence and interact with Hh and β -catenin signaling pathways in cartilage (37). Other genes whose levels correlated with *Ift88* included *Gli2*, *Ctgf*, and *Enpp1*, although these correlations were only statistically significant before Bonferroni correction.

While a gene expression analysis of microdissected mouse cartilage did not show a correlation between *Ift88* and classic Hh pathway molecules (*Gli1*, *Ptch1*), an individual cell analysis using RNAScope revealed increased levels of *Gli1* expression in *aggreCanCre^{ERT2};Ift88^{fl/fl}* mouse chondrocytes, suggesting a reciprocal relationship between Hh signaling and *Ift88*. Therefore, we propose that loss of *Ift88* disrupts ciliary-mediated repression of Hh signaling, resulting in net increases in *Gli1* expression. This is consistent with findings from previous studies in constitutive *Ift88* deletion (18) and endochondromas (43). In this model, our observation that cartilage atrophy was rescued and basal *Gli1* expression levels were normalized in *aggreCanCre^{ERT2};Ift88^{fl/fl}* mice following wheel exercise provides critical evidence of a link with mechanical loading. Our data imply that in postnatal mouse articular cartilage, ciliary protein IFT88 safeguards the progressive

mechanoadaptation of adolescent mouse cartilage, supporting the creation and maturation of fit-for-purpose adult mouse articular cartilage by ensuring appropriate levels of Hh signaling.

As previously described (44), *Ift88* was deleted in mouse chondrocytes using induction of Cre recombinase expression on the aggrecan promoter, which ensured sufficient expression in mice from adolescence through adulthood. Despite the use of this method, we observed only a 40% reduction in *Ift88*-positive chondrocytes in the tibial articular cartilage of *aggreCanCre^{ERT2};Ift88^{fl/fl}* mice. Observations in the tdTomato reporter line of mice indicated that *Ift88* deletion occurred in only a small proportion of chondrocytes, but this was not exclusive to any knee compartment, and therefore it is unlikely that this finding could be attributed to differences between the medial and lateral sides of the knee joint. We also recognize that, due to the challenges associated with imaging cilia in cartilage, we have not yet been able to address the question of whether primary cilia would be negatively impacted as a result of *Ift88* deletion. Thus, we cannot conclude that molecular changes are a direct consequence of the loss of cilia. To date, we have not yet conducted experiments inducing *Ift88* deletion in mice older than age 8 weeks to evaluate whether this gene is as influential later in adulthood, or assessed how behavior of the *aggreCanCre^{ERT2};Ift88^{fl/fl}* mice could be altered.

In summary, these data demonstrate that IFT88 is highly influential in adolescent mouse and adult mouse articular cartilage as a positive regulator of cartilage thickness, guiding cartilage calcification during maturation and safeguarding physiologic Hh signaling in adult mouse cartilage in response to mechanical cues.

AUTHOR CONTRIBUTIONS

All authors were involved in drafting the article or revising it critically for important intellectual content, and all authors approved the final version to be published. Dr. Coveney had full access to all of the data in the study and takes responsibility for the integrity of the data and the accuracy of the data analysis.

Study conception and design. Coveney, Wann.

Acquisition of data. Coveney, Zhu, Miotla-Zarebska, Chang, McSorley.

Analysis and interpretation of data. Coveney, Stott, Parisi, Batchelor, Duarte, Vincent, Wann.

REFERENCES

- Simon WH. Scale effects in animal joints. I. Articular cartilage thickness and compressive stress. *Arthritis Rheum* 1970;13:244–56.
- Grodzinsky AJ, Levenston ME, Jin M, Frank EH. Cartilage tissue remodeling in response to mechanical forces [review]. *Annu Rev Biomed Eng* 2000;2:691–713.
- Palmoski MJ, Brandt KD. Effects of static and cyclic compressive loading on articular cartilage plugs in vitro. *Arthritis Rheum* 1984;27:675–81.
- Osborne AC, Lamb KJ, Lewthwaite JC, Dowthwaite GP, Pittsillides AA. Short-term rigid and flaccid paralyses diminish growth of embryonic chick limbs and abrogate joint cavity formation but differentially preserve pre-cavitated joints. *J Musculoskelet Neuronal Interact* 2002;2:448–56.

5. Palmoski M, Perricone E, Brandt KD. Development and reversal of a proteoglycan aggregation defect in normal canine knee cartilage after immobilization. *Arthritis Rheum* 1979;22:508–17.
6. Vincent TL, Wann AK. Mechanoadaptation: articular cartilage through thick and thin [review]. *J Physiol* 2019;597:1271–81.
7. Vincent TL, Hermansson MA, Hansen UN, Amis AA, Saklatvala J. Basic fibroblast growth factor mediates transduction of mechanical signals when articular cartilage is loaded. *Arthritis Rheum* 2004;50:526–33.
8. Lin AC, Seeto BL, Bartoszko JM, Khoury MA, Whetstone H, Ho L, et al. Modulating hedgehog signaling can attenuate the severity of osteoarthritis. *Nat Med* 2009;15:1421–5.
9. Tang X, Muhammad H, McLean C, Miotla-Zarebska J, Fleming J, Didangelos A, et al. Connective tissue growth factor contributes to joint homeostasis and osteoarthritis severity by controlling the matrix sequestration and activation of latent TGF β . *Ann Rheum Dis* 2018;77:1372–80.
10. Wu Q, Zhang Y, Chen Q. Indian hedgehog is an essential component of mechanotransduction complex to stimulate chondrocyte proliferation. *J Biol Chem* 2001;276:35290–6.
11. Poole CA, Jensen CG, Snyder JA, Gray CG, Hermanutz VL, Wheatley DN. Confocal analysis of primary cilia structure and colocalization with the Golgi apparatus in chondrocytes and aortic smooth muscle cells. *Cell Biol Int* 1997;21:483–94.
12. Bangs F, Anderson KV. Primary cilia and mammalian hedgehog signaling [review]. *Cold Spring Harb Perspect Biol* 2017;9:a028175.
13. Whewey G, Nazlamova L, Hancock JT. Signaling through the primary cilium. *Frontiers Cell Dev Biol* 2018;6:8.
14. Praetorius HA, Frokiaer J, Nielsen S, Spring KR. Bending the primary cilium opens Ca $^{2+}$ -sensitive intermediate-conductance K $^{+}$ channels in MDCK cells. *J Membr Biol* 2003;191:193–200.
15. Wann AK, Zuo N, Haycraft CJ, Jensen CG, Poole CA, McGlashan SR, et al. Primary cilia mediate mechanotransduction through control of ATP-induced Ca $^{2+}$ signaling in compressed chondrocytes. *FASEB J* 2012;26:1663–71.
16. Coveney CR, Collins I, McFie M, Chanalaris, Yamamoto K, Wann AK. Cilia protein IFT88 regulates extracellular protease activity by optimizing LRP-1-mediated endocytosis. *FASEB J* 2018;32:fj201800334.
17. Haycraft CJ, Zhang Q, Song B, Jackson WS, Detloff PJ, Serra R. Intraflagellar transport is essential for endochondral bone formation. *Development* 2007;134:307–16.
18. Chang CF, Ramaswamy G, Serra R. Depletion of primary cilia in articular chondrocytes results in reduced Gli3 repressor to activator ratio, increased Hedgehog signaling, and symptoms of early osteoarthritis. *Osteoarthritis Cartilage* 2012;20:152–61.
19. Yuan X, Yang S. Deletion of IFT80 impairs epiphyseal and articular cartilage formation due to disruption of chondrocyte differentiation. *PLoS One* 2015;10:e0130618.
20. Lo Cascio L, Liu K, Nakamura H, Chu G, Lim NH, Chanalaris A, et al. Generation of a mouse line harboring a Bi-transgene expressing luciferase and tamoxifen-activatable creER(T2) recombinase in cartilage. *Genesis* 2014;52:110–9.
21. Glasson SS, Askew R, Sheppard B, Carito B, Blanchet T, Ma HL, et al. Deletion of active ADAMTS5 prevents cartilage degradation in a murine model of osteoarthritis. *Nature* 2005;434:644–8.
22. Ismail HM, Miotla-Zarebska J, Troeberg L, Tang X, Stott B, Yamamoto K, et al. JNK2 controls aggrecan degradation in murine articular cartilage and the development of experimental osteoarthritis. *Arthritis Rheumatol* 2015;68:1165–71.
23. Little CB, Barai A, Burkhardt D, Smith SM, Fosang AJ, Werb Z, et al. Matrix metalloproteinase 13-deficient mice are resistant to osteoarthritic cartilage erosion but not chondrocyte hypertrophy or osteophyte development. *Arthritis Rheum* 2009;60:3723–33.
24. Nalesso G, Thomas BL, Sherwood JC, Yu J, Addimanda O, Eldridge SE, et al. WNT16 antagonises excessive canonical WNT activation and protects cartilage in osteoarthritis. *Ann Rheum Dis* 2017;76:218–26.
25. Mak KK, Kronenberg HM, Chuang PT, Mackem S, Yang Y. Indian hedgehog signals independently of PTHrP to promote chondrocyte hypertrophy. *Development* 2008;135:1947–56.
26. Benichou C, Wirotius JM. Articular cartilage atrophy in lower limb amputees. *Arthritis Rheum* 1982;25:80–2.
27. Palmoski MJ, Brandt KD. Running inhibits the reversal of atrophic changes in canine knee cartilage after removal of a leg cast. *Arthritis Rheum* 1981;24:1329–37.
28. Koyama E, Young B, Nagayama M, Shibukawa Y, Enomoto-Iwamoto M, Iwamoto M, et al. Conditional Kif3a ablation causes abnormal hedgehog signaling topography, growth plate dysfunction, and excessive bone and cartilage formation during mouse skeletogenesis. *Development* 2007;134:2159–69.
29. Rockel JS, Yu C, Whetstone H, Craft AM, Reilly K, Ma H, et al. Hedgehog inhibits β -catenin activity in synovial joint development and osteoarthritis. *J Clin Invest* 2016;126:16–63.
30. Jin Y, Cong Q, Gvozdenovic-Jeremic J, Hu J, Zhang Y, Terkeltaub R, et al. Enpp1 inhibits ectopic joint calcification and maintains articular chondrocytes by repressing hedgehog signaling. *Development* 2018;145:dev164830.
31. Frost HM. The mechanostat: a proposed pathogenic mechanism of osteoporoses and the bone mass effects of mechanical and nonmechanical agents [review]. *Bone Miner* 1987;2:73–85.
32. Nauli SM, Alenghat FJ, Luo Y, Williams E, Vassilev P, Li X, et al. Polycystins 1 and 2 mediate mechanosensation in the primary cilium of kidney cells. *Nat Gen* 2003;33:129–37.
33. McGlashan SR, Haycraft CJ, Jensen CG, Yoder BK, Poole CA. Articular cartilage and growth plate defects are associated with chondrocyte cytoskeletal abnormalities in Tg737orpk mice lacking the primary cilia protein polaris. *Matrix Biol* 2007;26:234–46.
34. Chang CF, Serra R. Ift88 regulates hedgehog signaling, Sfrp5 expression, and β -catenin activity in post-natal growth plate. *J Orthop Res* 2013;31:350–6.
35. Huber C, Cormier-Daire V. Ciliary disorder of the skeleton [review]. *Am J Med Genet C Semin Med Genet* 2012;160c:16–74.
36. Wang C, Yuan X, Yang S. IFT80 is essential for chondrocyte differentiation by regulating hedgehog and Wnt signaling pathways. *Exp Cell Res* 2013;319:623–32.
37. Rockel JS, Yu C, Whetstone H, Craft AM, Reilly K, Ma H, et al. Hedgehog inhibits β -catenin activity in synovial joint development and osteoarthritis. *J Clin Invest* 2016;126:1649–63.
38. Clement CA, Larsen LA, Christensen ST. Using nucleofection of siRNA constructs for knockdown of primary cilia in P19.CL6 cancer stem cell differentiation into cardiomyocytes. *Methods Cell Biol* 2009;94:181–97.
39. Wann AK, Chapple JP, Knight MM. The primary cilium influences interleukin-1 β -induced NF κ B signalling by regulating IKK activity. *Cell Signal* 2014;26:1735–42.
40. McFie M, Koneva L, Collins I, Coveney CR, Clube AM, Chanalaris A, et al. Ciliary proteins specify the cell inflammatory response by tuning NF κ B signaling, independently of primary cilia. *J Cell Sci* 2020;133:jcs239871.
41. Anvarian Z, Mykityn K, Mukhopadhyay S, Pedersen LB, Christensen ST. Cellular signalling by primary cilia in development, organ function and disease [review]. *Nat Rev Nephrol* 2019;15:199–219.
42. Petrova R, Joyner AL. Roles for hedgehog signaling in adult organ homeostasis and repair [review]. *Development* 2014;141:3445–57.
43. Ho L, Ali SA, Al-Jazrawi M, Kandel R, Wunder JS, Alman BA. Primary cilia attenuate hedgehog signalling in neoplastic chondrocytes. *Oncogene* 2013;32:5388–96.
44. Nagao M, Cheong CW, Olsen BR. Col2-Cre and tamoxifen-inducible Col2-CreER target different cell populations in the knee joint. *Osteoarthritis Cartilage* 2016;24:188–91.